Coherent oscillations between classically separable quantum states of a superconducting loop

Vladimir E. Manucharyan,[1] Jens Koch,[1] Markus Brink,[1]

Leonid I. Glazman,[1] and Michel H. Devoret[1]

[1]*Departments of Physics and Applied Physics,*

Yale University, New Haven, Connecticut USA

Ten years ago, coherent oscillations between two quantum states of a superconducting circuit differing by the presence or absence of a single Cooper pair on a metallic island were observed for the first time[1]. This result immediately stimulated the development of several other types of superconducting quantum circuits behaving as artificial "atoms"[2,3,4,5,6], thus bridging mesoscopic and atomic physics. Interestingly, none of these circuits fully implements the now almost 30 year old proposal of A. J. Leggett[7] to observe coherent oscillations between two states differing by the presence or absence of a single fluxon trapped in the superconducting loop interrupted by a Josephson tunnel junction. This phenomenon of reversible quantum tunneling between two classically separable states, known as Macroscopic Quantum Coherence (MQC), is regarded crucial for precision tests of whether macroscopic systems such as circuits fully obey quantum mechanics[8,9]. In this article, we report the observation of such oscillations with sub-GHz frequency and quality factor larger than 500. We achieved this result with two innovations. First, our ring has an inductance four orders of magnitude larger than that considered by Leggett, combined with a junction in the charging regime[10], a parameter choice never addressed in previous experiments[11]. The higher the inductance and the smaller the capacitance of the small junction, the smaller the sensitivity of the spectrum of the "atom" to variations in the externally applied flux in the ring. Second, readout is performed with a novel dispersive scheme which eliminates the electromagnetic relaxation process induced by the measurement circuit (also known as Purcell effect[12]). Moreover, the reset of the system to its ground state is naturally built into this scheme, working even if the transition energy is smaller than that of temperature fluctuations. As we argue in this article, the MQC transition could therefore be, contrary to expectations, the basis of a superconducting qubit of improved coherence and readout fidelity.

When Anthony Leggett wrote in 1980: "[...] at the time of writing I am inclined to believe that it will turn out to be impossible in practice (at least in the near future) to see 'full-blooded' coherence between states [of a Radio Frequency (RF)-SQUID] differing by a full flux quantum..."[7], two major decoherence sources seemed very difficult to circumvent: (i) Damping of the MQC oscillations by the readout circuitry and (ii) noise in the magnetic flux threading the loop. The spontaneous transition rate between two states $|0\rangle$ and $|1\rangle$ of a Josephson junction, induced by its coupling to the total admittance $Y(\omega)$ of the electromagnetic environment between the junction terminals, is given by $\Gamma_{1\to0} = 2\left|\langle 0|\hat{\varphi}|1\rangle\right|^2 R_Q \mathrm{Re}[Y(\omega_{01})]\,\omega_{01}$[13], where $R_Q = \frac{\hbar}{(2e)^2} \simeq 1\,\mathrm{k\Omega}$ is the resistance quantum for Cooper pairs, and $\hat{\varphi}$ is the gauge invariant phase difference operator across the junction. For the two lowest energy states of a RF-SQUID biased at the half-flux-quantum sweet spot $\Phi_{\mathrm{ext}} = \Phi_0/2$, on which we concentrate in this work, the matrix element $\langle 0|\hat{\varphi}|1\rangle$ almost coincides with half the 2π-travel of phase in the classical limit. For magnetometry measurements of the phase state using a second SQUID, $\mathrm{Re}[Y(\omega)]$ tends to be of order $1/Z_{\mathrm{vac}}$, where $Z_{\mathrm{vac}} \simeq 377\,\Omega$ is the vacuum impedance, and since $R_Q > Z_{\mathrm{vac}}$ the coherence is very short lived[14,15]. Turning now to flux noise induced decoherence, even at the sweet spot, where first order effects vanish, a flux fluctuation $\delta\Phi_{\mathrm{ext}}$ will cause a variation in $\hbar\omega_{01}$ given by $\left(\delta\Phi_{\mathrm{ext}}\Phi_0/L\right)^2 / \left[\hbar\omega_{01}\left(\Phi_{\mathrm{ext}} = \Phi_0/2\right)\right]$ where L is the total inductance of the SQUID loop. Typical values of flux noise and loop inductance in RF-SQUIDs greatly reduce the coherence of these devices. Nevertheless, coherent oscillations in the three and four junction flux qubits were finally observed[4] and improved to a large extent[16], but at the expense of working with non-separable states, i.e. states with largely overlapping probability distributions, an aspect resulting from the large tunneling frequencies $\omega_{01}(\Phi_{\mathrm{ext}} = \Phi_0/2)$, typically exceeding $5\,\mathrm{GHz}$ in these experiments. In the novel fluxonium circuit[10], presented in Fig. 1 (a-c), both difficulties (i) and (ii) are remedied without sacrifying the key features of tunneling between separable states and the phase travel of 2π.

The equivalent electrical circuit of the fluxonium (Fig. 1d) consists of a small junction with Josephson inductance L_J and capacitance C_J shunted by an inductance L provided by a series array of carefully chosen larger area tunnel junctions, which is approximately $10,000$ times more inductive than a wire of the same length ($20\,\mu\mathrm{m}$). In order to read the states of such circuit, an operation described in detail below, the junction is coupled via a capacitance C_c to a $L_R C_R$ harmonic oscillator implemented with a quarter-wave transmission line resonator (Fig. 1c). In the resulting "atom+cavity" system[17,18], the dynamical variables of the "atom" are the flux Φ across the inductance L[19], and its canonically conjugate variable Q, which coincides
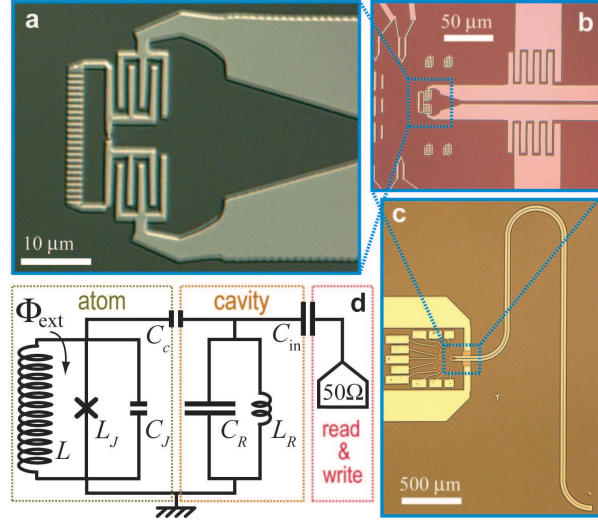
FIG. 1: **Fluxonium circuit. a-c** Optical photographs of the circuit at different scales. Panel **a** shows a loop consisting of a small junction shunted by an array of larger area junctions (oriented vertically) playing the role of an inductance. A pair of interdigitated capacitances couple the small junction to the end of a "parallel wires" (i.e. coupled microstrip) transmission line resonator. Panels **b** and **c** show the larger scale interdigitated capacitors which set the quality factor 400 of the resonator through the leakage of signals to the coupled microstrip 50 Ω measurement line. Panel **c** shows the entire snaked length of the quarter-wavelength resonator whose resonance frequency is 8.175 GHz. Also shown in this panel are test structures lying in the gap of the measurement line. Panel **d** represents the minimal circuit model of the device, which emulates an "atom+cavity" system. In this model, the array is represented as a single ideal inductance L while the distributed resonator is represented as a parallel combination of resonator inductance L_R and capacitance C_R, with resonance frequency $\omega_R = (L_R C_R)^{-1/2}$. The interdigitated capacitors are modelled by capacitances C_c and C_{in}. The coupling between the "atom" and the "cavity" is given by the linear interation term $g \frac{\hat{Q}}{2e} \left(a + a^\dagger \right)$ with the coupling constant $g = \omega_R \frac{C_c}{(C_J + C_c)} \sqrt{\frac{Z_R}{R_Q}} \simeq 2\pi \times 135$ MHz, Z_R being the oscillator impedance given by $\sqrt{L_R/C_R} \approx 80$ Ω. The device is placed in an external magnetic field and the applied flux threading the loop is Φ_{ext}, which is close to a half flux quantum $\Phi_0/2$.

here with the charge on the junction capacitance. Note that in contrast with the position and momentum of an electron in an ordinary atom, here the pair of variables Φ and Q describe the collective motion of a superconducting condensate around an entire circuit loop. Quantum-mechanically, these variables must be treated as operators satisfying $[\hat{\Phi}, \hat{Q}] = i\hbar$ and the cavity mode is described by annihilation and creation operators $\hat{a}$ and $\hat{a}^\dagger$ with $\left[\hat{a}, \hat{a}^\dagger \right] = 1$. The "atom"

is characterized by the three energies measured in a previous experiment on the same device but near zero external field: the Josephson energy $E_J/h = \frac{1}{h}(\Phi_0/2\pi)^2/L_J = 8.9$ GHz, the Coulomb charging energy $E_C/h = \frac{1}{h}\frac{1}{2}e^2/(C_J + C_c) = 2.4$ GHz and the inductive energy $E_L/h = \frac{1}{h}(\Phi_0/2\pi)^2/L = 0.52$ GHz. A conservative estimate of the uncertainty in the values given here is 2%, 8% and 2%, respectively. These three energies place our circuit in a so far unexplored niche of Josephson devices where E_J/E_C is of order unity while E_J/E_L is much larger than unity (see Fig. 2a). In this niche, like in that of SQUID-like devices, charge noise is suppressed, but remarkably, the sensitivity of the spectrum to flux noise is also greatly reduced[20].

Before describing our measurement, let us discuss quantitatively the issue of state separability. When the loop is biased by an external flux close to the half-flux-quantum $\Phi_0/2$, the two lowest states $|0\rangle$ and $|1\rangle$ of the fluxonium are the symmetric and antisymmetric combination of the states $|L\rangle$ and $|R\rangle$ described by two real wavefunctions $\langle\Phi|L\rangle$ and $\langle\Phi|R\rangle$ plotted in Fig. 2b. They are localized at $\Phi = -\Phi_0/2$ and $\Phi = +\Phi_0/2$, which are the location of the left and right minima of the double well potential seen by the flux coordinate Φ, respectively. We consider the two states $|L\rangle$ and $|R\rangle$ classically separable because when in state $|L(R)\rangle$, the probability to find the system in the right (left) well is much less than unity, or in more quantitative terms $s = |\langle0|\Phi|1\rangle|^2/\sqrt{\sigma_L\sigma_R} \gg 1$ where $\sigma_\Psi^2 = \langle\Psi|\Phi^2|\Psi\rangle - \langle\Psi|\Phi|\Psi\rangle^2$; $s = 8.5$ in the present experiment. Time domain coherent oscillations between these two states of a superconducting loop qualify as the MQC phenomenon. An equivalent way to evaluate the degree of separability is to compare the MQC oscillation frequency ω_{01} with the frequency of classical oscillations in either well, given approximately by $\omega_{\text{Classical}} = \sqrt{8E_JE_C}/h$. In the present experiment the two frequencies $\omega_{01}/2\pi$ and $\omega_{\text{Classical}}/2\pi$ are predicted, with better than 10% accuracy, to be given by 353 MHz and 13.5 GHz, respectively. Let us note that the center of mass motion of an ammonia molecule undergoing coherent tunneling (inversion transition) is equally qualified as an oscillation between two classically separable states in the sense we have given above[21] (see also a closely related discussion of Hund's paradox[22]).

How does one go about measuring the MQC oscillations? Directly measuring the flux generated by the MQC states with a SQUID is not an option here, despite the maximal swing in Φ: the mutual inductance of the fluxonium loop to any other superconducting loop in the vicinity - typically a pH per μm of wire - would approximately be $10,000$ times smaller than the fluxonium loop inductance $L = 300$ nH. Moreover, the amplitude of the current generated in the loop by the MQC oscillations is only of order 1 nA, so that in the end only a flux oscillation
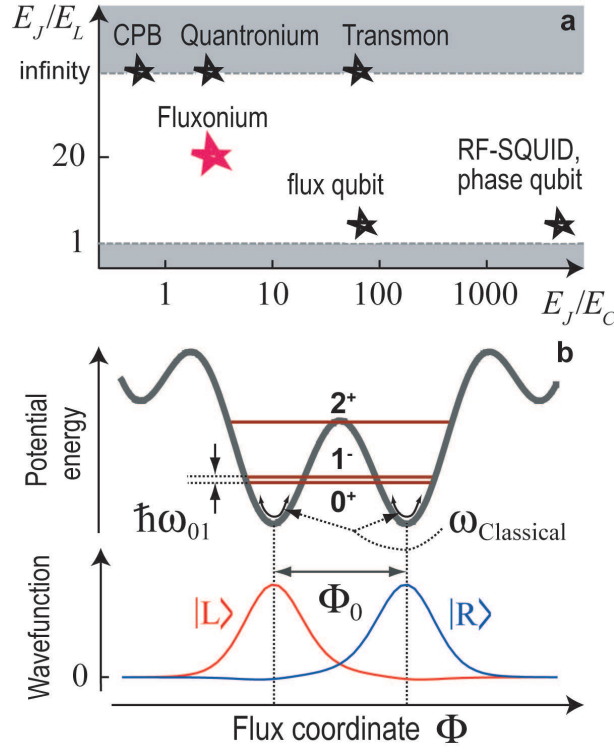
FIG. 2: **Specificity of fluxonium.** Panel **a** compares the parameters of the fluxonium artificial atom to that of other superconducting artificial atoms (qubits). For the Cooper pair box, quantronium and transmon, the effective inductance L can be considered infinite. The RF-SQUID and the phase qubits are represented by one star, because their parameters nearly coincide. For the flux qubit, the role of the shunting inductance can be thought of as that provided by the Josephson inductance of two or three larger junctions in series. Panel **b** shows the potential landscape seen by the flux coordinate Φ of the "atom" of Fig. 1 for $\Phi_{\text{ext}} = \Phi_0/2$. The two lowest minima, separated by a barrier and spanning a flux quantum, define two classically separable states. A necessary condition for their existence is $E_J/E_L > 1$. Such states, in the classical limit of $h \to 0$ correspond to vibrations near the bottoms of the minima with the characteristic frequency $\omega_{\text{Classical}}$. The splitting between the two lowest quantum levels (0^+ and 1^-) is due to reversible quantum tunneling through the barrier and define the "macroscopic quantum tunneling" frequency ω_{01}. The wavefunctions for the levels 0^+ and 1^- are symmetric and antisymmetric superpositions of the $|L\rangle$ (left) and $|R\rangle$ (right) wavefunctions plotted in the lower half of the panel. The latter two wavefunctions barely overlap under the barrier, indicating that tunneling is strongly suppressed. The third level (2^+) lies above the barrier and the transition 1-2, whose frequency is of order $\omega_{\text{Classical}}$ and about 30 times larger than that of transition 0-1, is used for reading out which of levels 0^+ and 1^- is occupied.

of $10^{-5}\Phi_0$ would be measured by a readout SQUID. We have circumvented these problems by a capacitive measurement scheme that exploits the presence of the second excited state, which lies slightly above the barrier of the double well (see Fig. 2b). The resonator frequency ω_R is chosen to be close to the 1-2 transition frequency of the atom, and their interaction provides a way to monitor dispersively the atomic 0-1 transition, as we show below. This new type of superconducting qubit readout shares common features with recent optical QND preparation and readout of spin-squeezed hyperfine clock states of Rb and Cs atoms[23,24]. Remarkably, the large separation of the cavity and qubit transition frequencies, $\omega_{01} \ll \omega_{12}, \omega_R$, forbids in our scheme the spontaneous emission of a photon from the qubit first excited state into the cavity (Purcell effect). In other words, $\mathrm{Re}[Y(\omega_{01})]$ is minimized without jeopardizing the readout fidelity.

We now turn to the two-tone spectroscopy results presented in Fig. 3a. They were obtained by applying a fixed frequency readout tone at the cavity frequency, and measuring the phase of the reflected readout signal as a function of the frequency of a second tone exciting the atomic transitions[25]. The flux dependence of all transition frequencies of the combined "atom+cavity" system agrees perfectly with theoretical predictions based on five adjustable parameters. The states are labeled with two numbers, the first referring to the atomic excitation and the second referring to the cavity excitation. We observe the atomic transitions 00-10, 10-20 and 00-20, as well as the red and blue sidebands involving both atom and cavity (10-01 and 00-11). In the same panel, a straight grey fuzzy line correspond to the measurement of the cavity response, obtained by single tone spectroscopy. This data notably displays the novel strong interaction regime of coupling between states 02 and 11, which manifests itself by the avoidance of the transitions 00-11 and 00-20 at the frequency of about 10 GHz. The minimum splitting $2g_{12}$ equals 130 MHz. At the same time, the MQC transition 00-10 located far down is surprizingly well resolved, with a power-broadened linewidth of about 3 MHz, as shown in the fine-scale spectroscopy data of the panels c) and d). The transition frequency passes through a minimum at half-flux quantum and the absolute measured value (368.9 ± 0.3) MHz of this lowest frequency through a Lorentzian fit is in agreement with theoretical predictions, within error bars.

To explain how the MQC transition, so highly detuned from the cavity, could be observed at all, we examine the minimal set of five levels represented in Fig. 3b for the coupled "atom+cavity" system. Two particular values of flux have been chosen, corresponding to arrows (i) and (ii) in panel a. At the point of maximum coupling (i), the states 20 and 11 have completely hybridized, while at the half-flux-quantum sweet spot (ii), where the hybridization is greatly reduced, they still repel significantly, producing a shift $\chi = \omega_{00 \longrightarrow 01} - \omega_{10 \longrightarrow 11}$ of the
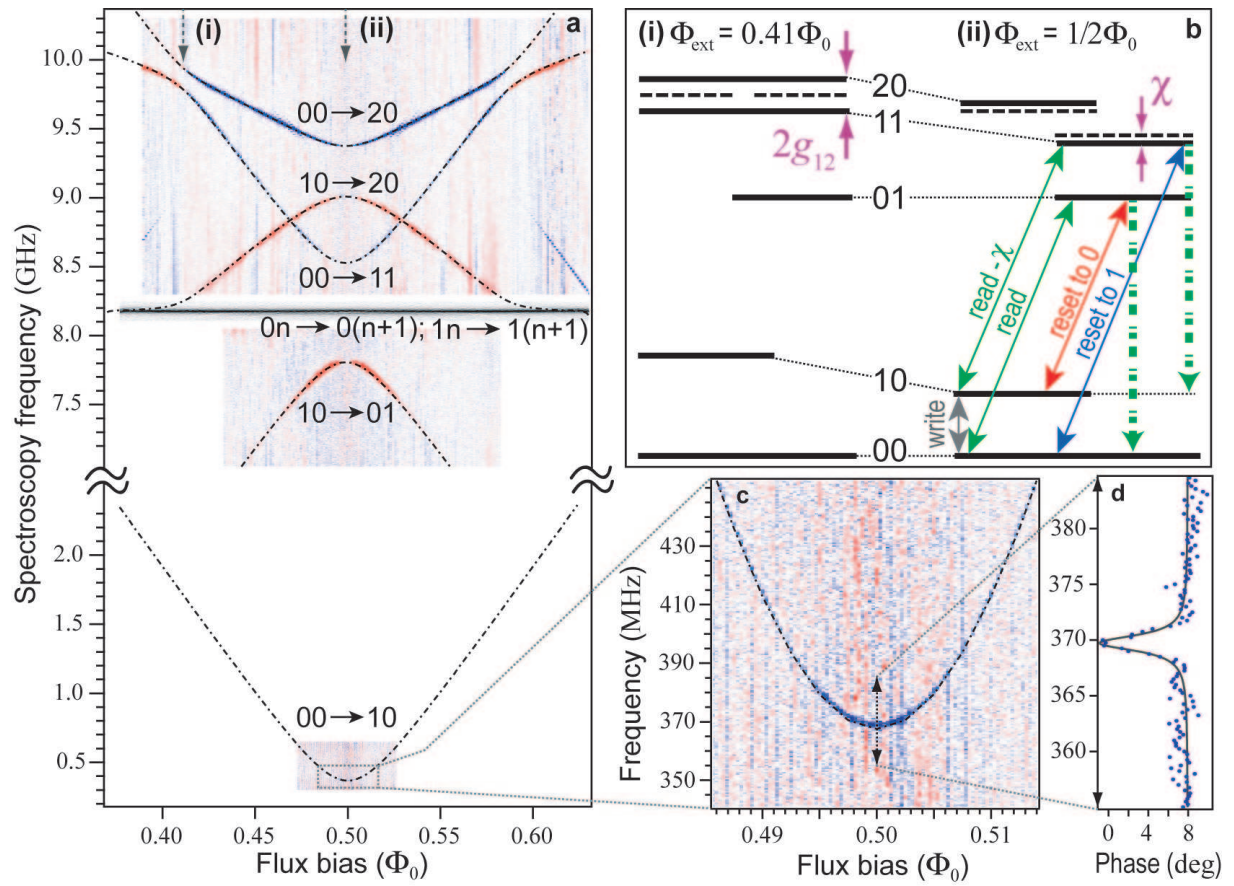
FIG. 3: **Two-tone spectroscopy.** Panel **a** shows the phase of the reflected readout tone as a function of the spectroscopy tone frequency and external flux. The color scale encodes the value of the phase, with zero corresponding to the mauve background, blue to negative values (dips), and red to positive values (peaks). The gray region around 8.2 GHz shows the reflected phase of a single tone, swept close to the resonator bare frequency. Theoretical predictions are shown in dot-dash lines. Transition assignments are indicated with a two-digit code, the first digit corresponding to the atom state and the second digit corresponding to the cavity photon number, as clarified in panel **b**, which shows the various functions of the irradiations used in the experiment. In that latter panel, the combined atom-cavity levels are shown for two special values of flux bias: the 11-20 degeneracy point (i) and the half flux quantum sweet spot (ii). Dashed lines indicate levels 11 and 20 in the absence of atom-cavity interaction. Panels **c** and **d** expand the sub-GHz MQC transition (00-10) observed in the vicinity of the sweet spot.

cavity frequency conditioned by the excitation of the atom in its 1 state. To second order in g, $\chi = (g_{12})^2 / (\omega_{12} - \omega_R) \simeq 10$ MHz. Thus, it is possible to read out the atom state by irradiating the system at the cavity frequency. In addition, by irradiating the red and blue sidebands, we can reset the qubit to either state 0 and 1. For instance, in the case of red sideband irradiation,

we are transferring a quantum of excitation from the qubit to the resonator, which in turn emits its energy into the $50\ \Omega$ input impedance of the readout amplifier. This important built-in reset feature suppresses the usual qubit requirement $k_B T \ll \hbar\omega_{01}$. Both the readout and reset manipulations are based on the fact that the relaxation rate of the cavity is much faster than the relaxation rate of the excited state involved in the MQC transition, i.e. $\kappa \gg \Gamma_{01}$.

Measurements in the time domain are performed by applying the protocol described in Fig. 3b(ii). A reset pulse is first applied to initialize the MQC doublet in either ground or excited state, and then a Rabi drive pulse is applied to write a given superposition state. The results are shown in Fig. 4a. When initialized in what is supposed to be the ground state, the system displays Rabi oscillations with a contrast increased relative to the thermal equilibrium value by a factor of 2, consistent with the estimated temperature of the sample. A reversal of the phase of Rabi oscillations is clearly observed when we now reset the system to what is supposed to be the 1 state. However, the contrast of the oscillations is found to be weaker than for the reset to 0, a discrepancy which we attribute to the fact that reset requires such power that spurious transitions are likely to occur since sideband transitions is nearly forbidden at our working point, which was about 0.05% away from the half-flux quantum symmetry point.

Finally, the coherence of the MQC oscillation is measured using the Ramsey fringe protocol, as shown in Fig. 4b. After a reset pulse to the ground state, two $\pi/2$ pulses separated by a free-evolution waiting time are applied to the sample. The protocol ends with a final measurement pulse. We have taken this data for different drive frequencies as shown in the inset, confirming that the beating frequency f_{Ramsey} is correctly related to the drive frequency of our $\pi/2$ pulses. The fringes have a Gaussian decay envelope with a characteristic decay time of $T_{\mathrm{Ramsey}} = 250$ ns, corresponding to a coherence quality factor $Q_{MQC} = T_{\mathrm{Ramsey}}\omega_{01} = 580$. At the times corresponding to the extrema of the fringes, the systems is passing through the classically separable states $|L\rangle$ and $|R\rangle$. The decay time of the fringes is much shorter than the relaxation time $T_1 > 5\ \mu$s, obtained in a separate experiment. At the time of this writing, we do not yet have an explanation for this short coherence time: At the transition frequency minimum, simple predictions based on the $10^{-6}\Phi_0/\left(\mathrm{Hz}\right)^{1/2}$ @1 Hz $1/f$ flux noise limitations observed at larger flux bias and treated here to second order, as well as estimates based on critical current $1/f$ noise fluctuations $10^{-6}I_0/\left(\mathrm{Hz}\right)^{1/2}$ @1 Hz[26] of the small junction give $T_{\mathrm{Ramsey}} > 10$ ms and $T_{\mathrm{Ramsey}} > 100\ \mu$s, respectively. Another concern would be fluctuations in the value of the inductance of the array; however $d\omega_{01}/dL$ is minimal at half-flux-quantum whereas measured coherence improves away from this point. Further experiments are clearly needed to explore
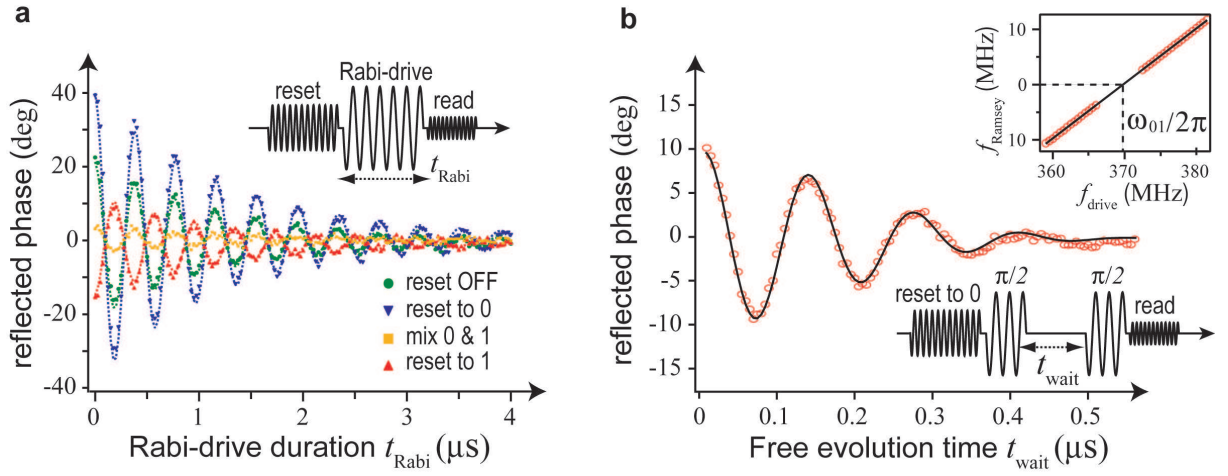
FIG. 4: **Observation of MQC in the time domain.** Panel **a** shows Rabi oscillations between ground (0) and first excited state (1) of the qubit, measured for different qubit initialization protocols. Green dots: wait for thermal equibilibrium no reset. Blue/Red triangle: reset to 0/1 applied (10-01/00-11 transition in Fig. 3b). Yellow squares: reset-to-1 pulse of weaker amplitude applied to nearly maximally mix states 0 and 1. Panel **b** shows Ramsey fringe after initialization to ground state, with inset giving Ramsey beating frequency as a function of qubit drive frequency. The fringes correspond to stroboscopy of MQC oscillations between states $|L\rangle$ and $|R\rangle$.

other hypotheses like out-of-equilibrium quasiparticles or quantum phase slips in the junction array[27] resulting in decoherence from charge noise. Both of these mechanisms could be remedied: quasiparticle traps could be added and phase slips could be suppressed by a slight increase in the array junction size. Furthermore by using the device in clusters[28], a system with a topologically protected doublet ground state could in principle be implemented, in order to suppress more completely the effect of decoherence[29].

In conclusion, we have reported the first observation, in the time domain, of the reversible tunneling of the macroscopic superconducting phase difference between two wells of the Josephson potential. In contrast with experiments on RF-SQUIDs and flux qubits, the total phase travel is 2π while the standard deviation of the probability distribution at the oscillation extrema is much less than π. The oscillation coherence factor, although surprisingly good in view of initial expectations, is much lower than what an analysis based on typical levels of noise encountered in this type of superconducting device predicts. Therefore, the coherence is likely to improve and this new device would become a very promising qubit that, while easy to read and to reset, escapes from the limitations of the Purcell effect: because the frequency of this

qubit is one order of magnitude smaller than that of other superconducting qubits, the control of noise and dissipation in a reduced frequency range might be easier to realize, while the time to perform a two-qubit gate would not be slowed down. Even smaller frequencies are worth exploring, since there is no limitation on the possibility of artificially resetting the system in its ground state. These lower frequencies would allow a coupling to nanomechanical systems[30] which themselves are interfacable to light beams for the transport of quantum information. On a more fundamental level, our experiment on a fluxonium version of the MQC system confirms its status as a testing ground for eventual limitations of quantum mechanics, since it is one of the very few that lends itself to a controlled, absolute measurement of anomalies in the vanishing reversible tunneling rate between two classically separable macroscopic states.

---

1. Nakamura, Y., Pashkin, Yu. A., Tsai, J. S. Coherent control of macroscopic quantum states in a single-Cooper-pair box. *Nature* **398**, 786-788 (1999).

2. Vion, D. et al. Manipulating the Quantum State of an Electrical Circuit. *Science* **296**, 886-889 (2002).

3. Martinis, J. M., Nam, S., Aumentado, J., Urbina, C. Rabi oscillations in a large Josephson-junction qubit. *Phys. Rev. Lett.* **89**, 117901 (2002).

4. Chiorescu, I., Nakamura, Y., Harmans, C. J. P. M., Mooij, J. E. Coherent Quantum Dynamics of a Superconducting Flux Qubit. *Science* **299**, 1869-1871 (2003).

5. Schreier, J. A. et al. Suppressing charge noise decoherence in superconducting charge qubits. *Phys. Rev. B* **77**, 180502(R) (2008).

6. Hoskinson, E. et al. Quantum Dynamics in a Camelback Potential of a dc SQUID. *Phys. Rev. Lett.* **102**, 097004 (2009).

7. Leggett, A. J. Macroscopic Quantum Systems and the Quantum Theory of Measurement. *Prog. Theor. Phys.*, suppl no. **69**, 80-100 (1980).

8. Leggett, A. J. Testing the limits of quantum mechanics: motivation, state of play, prospects. *J. Phys.: Condens. Matter* **14,** R415-R451 (2002).

9. Takagi, S. in *Macroscopic Quantum Tunneling,* (Cambridge Univ. Press, Cambridge, 2002).

10. Manucharyan, V. E., Koch, E., Glazman, L. I., Devoret, M. H. Fluxonium: Single Cooper-Pair Circuit Free of Charge Offsets. *Science*, **326**, 113-116 (2009).

11. *Exploring the Quantum/Classical Frontier* (eds. Friedman, J. R., Han, S.) (Nova Science Publishers, Inc, Hauppauge, 2003).

12. Purcell, E. M. Spontaneous Emission Probabilities at Radio-Frequencies. *Phys. Rev.* **69**, 681 (1946).

13. Schoelkopf, R. J., Clerk, A. A., Girvin, S. M., Lehnert, K. W., Devoret, M. H. in *Quantum Noise in Mesoscopic Systems* (ed. Nazarov, Yu. V.), 175-203 (Kluwer, Netherlands, 2003).

14. van der Wal, C. H. et al. Quantum Superposition of Macroscopic Persistent-Current States. *Science* **290**, 773-777 (2000).

15. Friedman, J. R., Patel, V., Chen, W., Tolpygo, S. K., Lukens, J. E. Quantum superposition of distinct macroscopic states. *Nature* **406**, 43-46 (2000).

16. Yoshihara, F. , Harrabi, K., Niskanen, A. O., Nakamura, Y., Tsai, J. S. Decoherence of Flux Qubits due to 1/f Flux Noise, *Phys. Rev. Lett.* **97**, 167001 (2006).

17. Raimond, J., Brune, M., Haroche, S. Colloquium: Manipulating quantum entanglement with atoms and photons in a cavity. *Rev. Mod. Phys.* **73**, 565-582 (2001).

18. Wallraff, A. et al. Strong coupling of a single photon to a superconducting qubit using circuit quantum electrodynamics. *Nature* **431**, 162-167 (2004).

19. Devoret, M. H. in *Quantum Fluctuations in Electrical Circuits* (eds. S.Reynaud, E. Giacobiano, J. Zinn-Justin) (Elsevier, Amsterdam, 1997).

20. Koch, J., Manucharyan, V. E., Devoret, M. H., Glazman, L. I. Charging effects in the inductively shunted Josephson junction. *Phys. Rev. Lett.* [in print]; http://arxiv.org/abs/0902.2980.

21. Bethlem, H. L., Kajita, M., Sartakov, B., Meijer, G., Ubachs, W. Prospects for precision measurements on ammonia molecules in a fountain. *Eur. Phys. J. Special Topics* **163**, 55–69 (2008).

22. Day, C. Month-long calculation resolves 82-year-old quantum paradox. *Physics Today*, **62**, 16-17 (2009).

23. Appel, L. et al. Mesoscopic atomic entanglement for precision measurements beyond the standard quantum limit. *PNAS* **106**, 10960-10965 (2009).

24. Schlier-Smith, M., Leroux, I., Vuletic, V. Reduced-Quantum-Uncertainty States of an Ensemble of Two-Level Atoms. http://arxiv.org/abs/0810.2582.

25. Schuster, D. I. et al. ac Stark Shift and Dephasing of a Superconducting Qubit Strongly Coupled to a Cavity Field. *Phys. Rev. Lett.* **94**, 123602 (2005).

26. Van Harlingen, D. J. et al. Decoherence in Josephson-junction qubits due to critical-current fluctuations. *Phys. Rev. B* **70**, 064517 (2004).

27. Matveev, K. A., Larkin, A. I., Glazman, L. I. Persistent Current in Superconducting Nanorings. *Phys.Rev. Lett.* **89**, 096802 (2002).

28. Gladchenko, S. et al. Superconducting nanocircuits for topologcally protected qubits. *Nature Phys.* **5**, 48-53 (2009).

29. Ioffe, L. B., Feigel'man, M. V. Possible realization of an ideal quantum computer in Josephson junction array. *Phys. Rev. B* **66**, 224503 (2004).

30. LaHaye, M. D., Suh, J., Echternach, P. M., Schwab, K. C., Roukes, M. L. Nanomechanical measurements of a superconducting qubit. *Nature* **459**, 960-964 (2009).